Chemistry–A European Journal
Research Article
doi.org/10.1002/chem.202203704
Chemistry Europe
European Chemical Societies Publishing
www.chemeurj.org

Phosphorus-Boron Multiple Bonding in the π Radical HBP

Lina Wang,*[a] Xin Jiang,[a] Guanjun Wang,[a] Xiaoqing Zeng,*[a] and Mingfei Zhou*[a]

Abstract: The HBP radical was generated via the reaction of laser ablated boron atom with PH_3 in a solid neon matrix, which is identified via IR spectroscopy with isotopic substitutions and quantum chemical calculations. The results show that HBP has a $^2\Pi$ electronic ground state with a short B–P bond. Bonding analysis indicates that besides an electron-sharing σ bond, there are two degenerate π bonding orbitals that are occupied by three electrons, resulting in a bond order of two and half between P and B. This is in sharp contrast to the bonding properties of the isovalent HNB, which was characterized to be a N≡B triply bonded σ radical with the unpaired electron locating on the B atom.

Introduction

Heteroatomic multiple bonds between group 13 and group 15 elements are of interest due to their valence isoelectronic relationship with C=C and C≡C bonds.[1] The polarity of such bonds, a result of the electronegativity difference between the elements of group 13 and group 15, imparts chemical characteristics to molecules that differ significantly from their carbon-containing analogues.[2] Despite of its electron deficiency, the lightest group 13 element boron is capable of forming B≡B triple bonds,[3] as well as multiple bonds with various elements.[1c] The first iminoborane HNBH was formed from the photolysis of $H_3B{\cdot}NH_3$ in an argon matrix.[4] Later on, HNBH and the HNB radical were produced by the reactions of laser-ablated B atoms with NH_3 in a solid noble gas matrix.[5] Both HNBH and HNB were characterized to have linear structures with B≡N triple bond character (Scheme 1). Note that the higher BN stretching frequency and larger force constant of HNB than HNBH indicate that the former contains a stronger B≡N bond. The first stable iminoborane *t*Bu–N≡B-C_6F_5 with a B≡N triple bond was synthesized in 1979 (Scheme 1).[6] Since then, numerous compounds containing B≡N triple bond with short B–N bond lengths (1.23 to 1.26 Å) have been synthesized and characterized.[7] In sharp contrast, the heavy analogues containing BP, [8] BAs[8d] and BSb[9] multiple bonds have been much less explored. Although compounds containing B=P double bonds have been reported (Scheme 1),[10] molecules with B≡P triple bond remain elusive. Recently, multiple bonds between B and Bi were identified in the linear clusters BiB_2O^- ([Bi≡B–B≡O]$^-$) and Bi_2B^- ([Bi=B=Bi]$^-$), which were produced by laser vaporization of a mixed B/Bi target and characterized by anion photoelectron spectroscopy.[11]

The chemistry of iminoboranes is dominated by the polarity of the B≡N bond due to the large electronegativity difference between N and B (N = 3.07, B = 2.01).[12] In contrast, B and P have very similar electronegativity (B = 2.01, P = 2.06), phosphinidene boranes should thus display significantly different reactivity. Unlike the linear iminoboranes, comprehensive theoretical studies of the XPBY (X, Y=H, HO, H_3C, H_3Si, X=F and Y=Cl) molecules predicted a bent geometry with X–P-B angles close to 90° and B–P bond lengths in the range of 1.72–1.78 Å (Scheme 1).[13] The unusual bent structures have stimulated debates on fundamental questions concerning the B–P bond orders in the XBPY compounds.[12,13] It was proposed that the bent structure results from the localization of the lone pair electrons at the phosphorus center, enforcing similar frontier molecular orbitals to the heavier group 14 alkyne analogues and resulting in a maximum P=B bond order of 2.[13a] On the contrary, according to the valence bond theory, recent theoretical studies concluded B≡P triple bond nature.[13b] Interpretation of the bent geometry for the XBPY compounds is mainly due to the coupling between the lone pair electrons in P–Y and the empty p orbital of boron.[13b] In contrast to these theoretical studies, there are still no experimental reports on the prototype BP multiple bonding molecules such as HBPH, HBP, and HPB.[14] Herein, we report the generation and spectroscopic detection of HBP, H_2BPH, and H_2BPH_2 in cryogenic neon matrix, and the BP multiple bonding properties in HBP and H_2BPH have been disclosed.

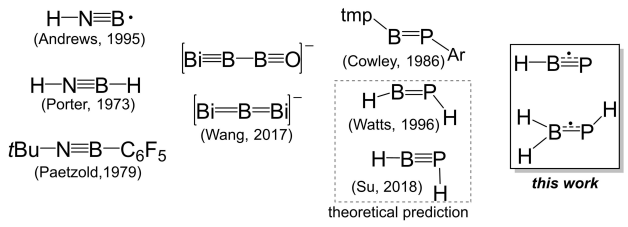

Scheme 1. Selected compounds containing multiple bonds between group 13 and group 15 elements (tmp = 2,2,6,6-tetramethylpiperidino; Ar = 2,4,6-(tBu)$_3$C$_6$H$_2$).

[a] *Dr. L. Wang, X. Jiang, Prof. G. Wang, Prof. X. Zeng, Prof. M. Zhou*
Department of Chemistry
Shanghai Key Laboratory of Molecular Catalysis and Innovative Materials
Fudan University
Shanghai 200433 (P. R. China)
E-mail: lina_wang@fudan.edu.cn
xqzeng@fudan.edu.cn
mfzhou@fudan.edu.cn

Supporting information for this article is available on the WWW under https://doi.org/10.1002/chem.202203704

Results and Discussion

The HBP and H_2BPH complexes were produced by the reaction of laser-evaporated boron atoms and PH_3 in solid neon matrix.[15] The infrared spectra in the 2750–2250 and 1175–950 cm^{-1} regions using an ^{10}B-enriched boron target and 0.2% PH_3/Ne sample are shown in Figure 1. After 30 min of sample deposition at 4 K, product absorptions (labeled as **A** and **B**) were observed. The absorptions of species **A** increase upon sample annealing to 11 K but decrease under irradiation at 625 nm. The absorptions of species **B** disappear under irradiation at 365 nm, while the absorption bands of species **C** appear. Reverse conversion of **C**→**B** can be induced by the irradiation at 625 nm. Similar experiments were performed with the isotopically labeled samples PD_3 and a naturally abundant boron target. The spectra are shown in Figure S1 of Supporting Information.

The group **A** absorptions are assigned to the fundamental vibrational modes of HBP (Table 1). The experiments using different isotopically-labeled mixture samples confirm that **A** contains only one B and one H atoms. The strongest band at 2708.5 cm^{-1} shows large ^{11}B (−13.8 cm^{-1}) and D (−649.2 cm^{-1}) isotopic shifts. The band position and isotopic shifts imply that it corresponds to a terminal B–H stretching vibration. The frequency is lower than those in BNBH (2826.9 cm^{-1}, Ar-matrix)[5a] and HBNH (2796.9 cm^{-1}, Ar-matrix),[5b] but is higher than those of HBBH (2691.3 cm^{-1}, Ar-matrix),[16] HB (2268.3 cm^{-1}, Ar-matrix),[5b] CH_3BH (2575.3 cm^{-1}, Ar-matrix),[17] and HBNCO (2574.1 cm^{-1}, Ne-matrix).[18] The band at 1008.3 cm^{-1} shows ^{11}B isotopic shift of −29.2 cm^{-1} and D isotopic shift of −65.5 cm^{-1} (Table 1), and can be assigned to the BP stretching vibration.

The identification of HBP is supported by the good agreement with the calculations at the B3LYP/6-311+G(3df) level of theory (Table 1). Besides the B–P and B–H stretching modes, the bending modes were calculated for $H^{10}BP$ at 654.1 and 620.6 cm^{-1} with low IR intensities of 8 and 7 km mol^{-1}, respectively, and they were not observed in the spectrum (Table S1). The *cyclic*-HBP and HPB isomers were also calculated.

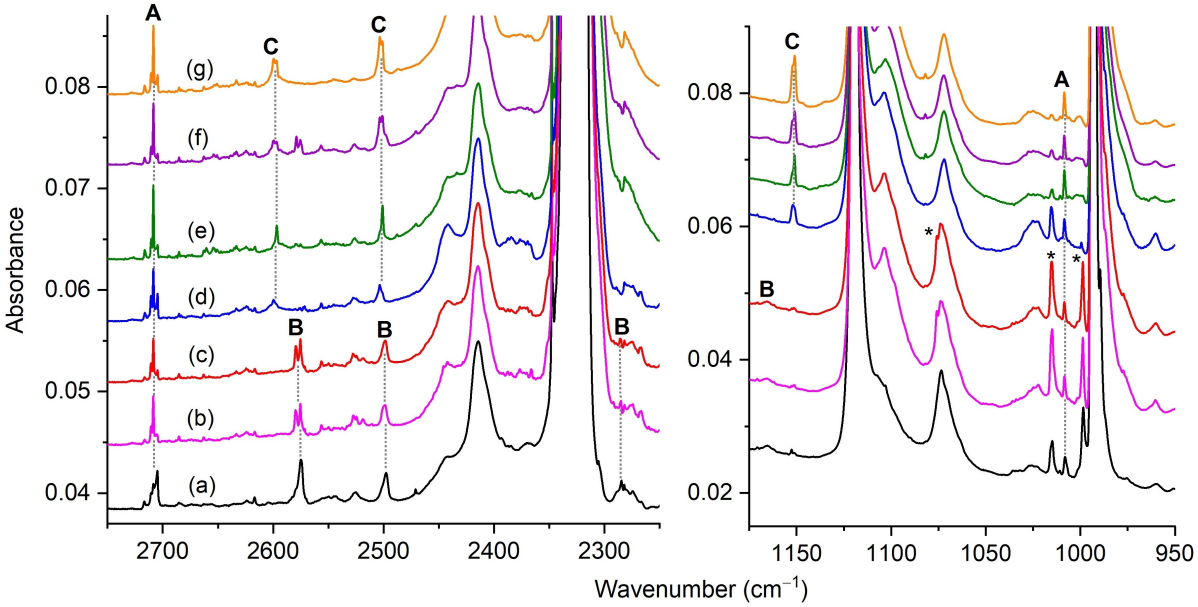

Figure 1. Infrared spectra in the 2750–2250 cm^{-1} and 1175–950 cm^{-1} regions from codeposition of laser-ablated ^{10}B-enriched boron atoms with 0.2% PH_3 in neon. a) 30 min of sample deposition at 4 K, b) 11 K annealing, c) 10 min of 625 nm irradiation, d) 5 min of 365 nm light irradiation, e) 11 K annealing, f) 15 min of 625 nm irradiation, and g) 5 min of 365 nm light irradiation. **A**: HBP, **B**: H_2BPH, **C**: H_2BPH_2, and unknown species ( ) are marked.

Table 1. Observed and calculated IR frequencies (cm^{-1}) and isotopic shifts ($\Delta\nu$, cm^{-1}) of HBP (**A**) and H_2BPH (**B**).

	Obs.[a] $^{10}B/PH_3$	$\Delta\nu(^{11}B)$	$\Delta\nu(D)$	Cal.[b] $^{10}B/PH_3$	$\Delta\nu(^{11}B)$	$\Delta\nu(D)$	Assignment
HBP[c]	2708.5	−13.8	−649.2	2714.7 (34)	−14.2	−673.4	ν(HB)
	1008.3	−29.2	−65.5	1000.9 (15)	−30.0	−48.1	ν(BP)
H_2BPH[c]	2578.8	−13.6	−620.4	2579.9 (85)	−14.7	−642.3	$\nu_{asym}(BH_2)$
	2498.2	−5.2	−709.6	2491.1 (80)	−5.4	−683.0	$\nu_{sym}(BH_2)$
	2285.1	0.0	n.o.[d]	2266.5 (40)	0.0	−638.8	ν(HP)
	1165.7	−7.3	n.o.	1136.1 (40)	−7.7	−256.3	$\delta(BH_2)$

[a] Observed band positions (cm^{-1}) in neon matrix at 4 K. [b] Calculated IR frequencies (cm^{-1}), intensities (km mol^{-1}, in parentheses) and isotopic shifts $\Delta\nu$ (cm^{-1}) at the B3LYP/6-311+G(3df) level. The calculated frequencies are scaled by a factor of 0.967. [c] The remaining unobserved frequencies for the calculations with low IR intensities are shown in Table S1, such as 654.1 (8) and 620.6 (7) for HBP and 930.0 (10), 716.9 (12), 632.0 (18), 555.1 (7) and 358.4 (7) for H_2BPH. [d] The abbreviation "n.o." denotes "not observed".

The former is a local minimum lying above the HBP isomer by 32.5 kcal mol^{-1}, while the latter is a transition state. The BHP deformation mode in *cyclic*-HBP at 716.0 cm^{-1} is the strongest mode (Table S2). The absence of this band in the spectrum precludes its formation in the experiment. Therefore, the reaction of B with PH_3 differs from the reaction with NH_3, since HNB rather than the less stable HBN was experimentally observed in the NH_3 experiments.[5b] We also calculated the UV-visible absorption spectrum of HBP at the TD–B3LYP/6-311+G(3df) level. The result shows that it has a strong absorption band at 593 nm (oscillator strength $f=0.0014$, Table S3) corresponding to the HOMO-1→LUMO transition, which is consistent with the experimental observation that the IR absorptions of HBP decrease under the irradiation at 625 nm.

Species **B** is assigned to H_2BPH, possibly formed from the B atom insertion into the P–H bond in PH_3 with subsequent intramolecular hydrogen-migration. The IR frequencies and isotopic shifts are listed in Table 1. The isotopic shifts clearly demonstrate that the bands at 2578.8 and 2498.2 cm^{-1} correspond to the BH_2 antisymmetric and symmetric stretching vibrations, respectively. The band at 1165.7 cm^{-1} with ^{11}B isotope shift of −7.3 cm^{-1} associates with the in-plane BH_2 deformation mode. Its D isotope shift is not resolved in the spectrum due to the overlap with the strong IR bands of the starting material in the range of 923.5–902.6 cm^{-1}. The band at 2285.1 cm^{-1} neighbours the IR band at 2328.0 cm^{-1} for PH_3 and exhibits no isotopic splitting with the naturally abundant boron target, which is indicative of a P–H stretching vibration. The assignment of the IR spectrum for H_2BPH is also supported by the agreement with the B3LYP/6-311+G(3df) calculations (Table 1). Note that H_2BPH possesses two chiral conformations with very similar IR features that are indistinguishable in our experiment (Figure S3). The less stable isomers $HBPH_2$ and BPH_3 were not observed (Table S4).

As shown in Figure 1, species **C** can interconvert with H_2BPH (**B**) under selective irradiations. The observed bands at 2599.7 cm^{-1}, 2503.6 cm^{-1} and 1152.3 cm^{-1} for **C** (Table S5) are quite close to those of 2578.8 cm^{-1}, 2498.2 cm^{-1}, and 1165.7 cm^{-1} for **B** with similar isotopic shifts. This strongly indicates that **C** has a similar structure with H_2BPH. The computed vibrational frequencies for the characteristic BH_2 moiety in the most likely candidate H_2BPH_2 are 2609.7 cm^{-1}, 2515.2 cm^{-1}, and 1155.0 cm^{-1} (Table S5), which nicely match to the aforementioned three bands for **C**. Due to the overlap with the IR bands for the reactant PH_3, the predicted IR bands of H_2BPH_2 at 2370.4, 2354.2 and 1083.5 cm^{-1} for the $\nu_{asym}(PH_2)$, $\nu_{sym}(PH_2)$ and $\delta(PH_2)$ modes could not be identified.

The optimized structure of HBP is shown in Figure 2. The calculations give a linear ($C_{\infty v}$) geometry with a B–P bond length of 1.719 Å, which lies between the standard values for a B–P triple bond (1.67 Å) and a B–P double bond (1.80 Å).[19] The Adaptive Natural Density Partitioning (AdNDP) analysis, which has the ability to recover simultaneously both localized and delocalized bonding in chemical species is performed. The results are shown in Figure 3. Besides the lone pair of phosphorus, there are one 2c–2e B–P σ bond, one 2c–2e π bond as well as one 2c–1e π bond. Accordingly, the B–P bond

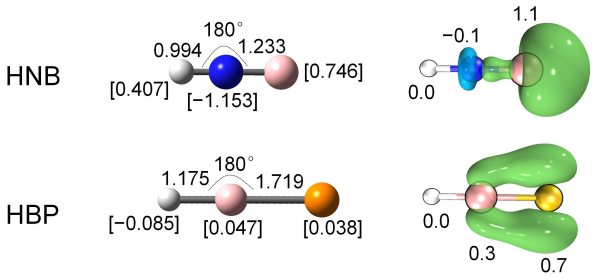

	MBO		WBO	
HNB	H–N	B–N	H–N	B–N
	0.70	2.34	0.78	3.30
HBP	H–B	B–P	H–B	B–P
	0.81	2.19	0.90	3.15

Figure 2. Top: Calculated equilibrium geometries (left panel) and spin density distributions (right panel) of HNB and HBP at the B3LYP/6-311+G(3df) level of theory. Bond lengths are in Å, bond angles are in degrees. The partial natural charges on each atom are given in square brackets. The natural spin density is given in e units. The isovalue is 0.003 au. Bottom: Calculated bond orders given by the Wiberg method (WBO) and the Mayer approach (MBO).

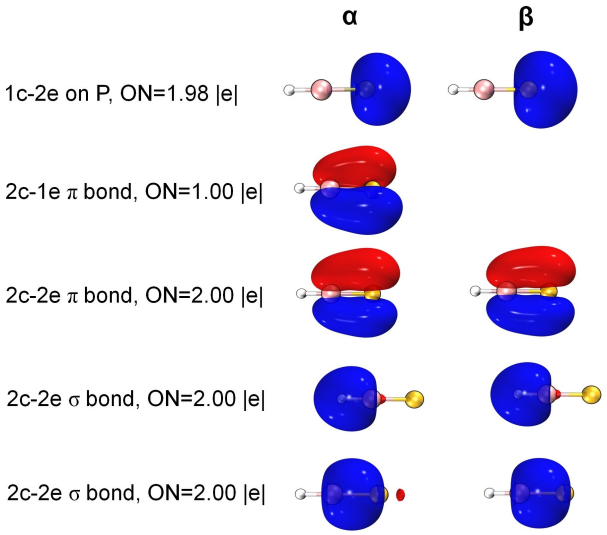

Figure 3. Chemical bonding pattern of HBP by the AdNDP analysis. ON stands for occupation number.

has a bond order of 2.5. The calculated bond orders defined by Wiberg[21] and by Mayer[22] are also shown in Figure 2. The Mayer and Wiberg bond orders were calculated to be 2.19 and 3.15, respectively, which are lower than the values for the B≡N triple bond in HNB (2.34 and 3.30). The first excited state of HBP ($A^2\Sigma^+$) with a linear structure was predicted to be higher in energy than the ground state by 1.97 eV at the B3LYP level.[20] It corresponds to an electronic configuration of $[1\sigma^2 2\sigma^2 3\sigma^2 4\sigma^2 1\pi^4 5\sigma^2 6\sigma^2 7\sigma^1 2\pi^4]$, which associates with a B≡P triple bond. The valence isoelectronic analogue HNB exhibits $^2\Sigma^+$ electronic ground state similar to the first excited state of HBP. The unpaired electron in HNB is located at the boron atom

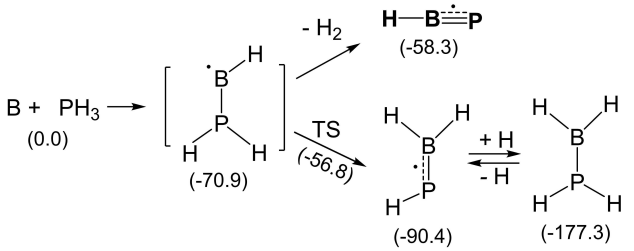

Scheme 2. Reaction mechanism for laser ablated boron atom with PH_3. Relative energies (kcal mol^{-1}) calculated at the B3LYP/6-311 + G(3df) level of theory are given in parentheses. The unpaired electron is represented by a dot.

(Figure 2), and the nitrogen lone pair is involved in bonding to boron giving a formal B≡N triple bond.

The H_2BPH (**B**) molecule was predicted to have a doublet ground state with a non-planar structure. The B–P bond length is 1.884 Å, which lies between the standard values for a B–P double bond (1.80 Å) and a B–P single bond (1.96 Å).[19] Bonding analysis with AdNDP method indicates that there is a B–P σ bond and a one-electron π bond (Figure S4). The calculated Mayer and Wiberg bond orders for B–P are 1.23 and 2.27, respectively, which are lower than the values of HBP (2.19 and 3.15) calculated at the same level of theory.

Scheme 2 outlines the possible pathways for the formation of the observed species in the reaction of B and PH_3. The insertion of B atom into a P–H bond requires activation energy, which can be provided by the laser ablated B atoms. The unobserved intermediate $HBPH_2$ contains large excess energy, which may either decompose to give HBP by H_2-elimiation (12.6 kcal mol^{-1}) or isomerize to the more stable isomer H_2BPH (−19.5 kcal mol^{-1}) through a barrier of 14.1 kcal mol^{-1}. Similar dehydrogenation from the PH_2 moiety has been reported for ethynylphosphine $HCCPH_2$, which leads to the formation of ethynylphosphinidene HCCP.[23] Note that elimination of one hydrogen atom from $HBPH_2$ to generate HBPH requires more energy input (39.3 kcal mol^{-1}) than the aforementioned H_2-elimiation (12.6 kcal mol^{-1}), which may explain the absence of HBPH in the experiment. The observation here differs from the reactions between laser-ablated B and NH_3, in which product species including $HBNH_2$, HBNH and HNB were produced. It mainly results from the stronger bond of H–N (D^0_{298} = 338.9 kJ mol^{-1}) than H–P (D^0_{298} = 297.0 kJ mol^{-1}).[24]

Conclusions

In summary, the elusive π-radical HBP along with H_2BPH and H_2BPH were generated via the reactions of laser-ablated B atoms with PH_3 in solid neon, which were characterized by IR spectroscopy and quantum-chemical calculations. The HBP molecule possesses a linear structure with the unpaired electron occupying one of the doubly degenerate π bonding MOs, resulting in a B–P bond order of 2.5. The bonding property is distinct from the valence isoelectronic analogue HNB, which is a σ-radical with a formal N≡B triple bond.

Experimental Section

The 1064 nm fundamental of a Nd:YAG laser (Continuum, Minilite II, 10 Hz repetition rate and 6 ns pulse width) was used to ablate rotating bulk boron target to produce boron atoms. The laser-evaporated boron atoms were co-deposited with premixed PH_3 in excess neon onto a cryogenic gold-plated copper block matrix support, which was maintained at 4 K by means of a closed-cycle helium refrigerator. The PH_3/Ne mixtures were prepared in a stainless-steel vacuum line by using a standard manometric technique. Natural-abundance boron (19.8% ^{10}B, 80.2% ^{11}B) and ^{10}B-enriched (97%) targets were used in different experiments. After 30 min of sample deposition at 4 K, IR absorption spectra in the middle-infrared region (4000-500 cm^{-1}) were recorded with a Bruker Vertex 70 V spectrometer at 0.5 cm^{-1} resolution using a liquid nitrogen cooled broad band HgCdTe (MCT) detector. Bare mirror backgrounds, recorded prior to sample deposition were used as references in processing the sample spectra. The spectra were subjected to baseline correction to compensate for infrared light scattering and interference patterns. Samples were annealed to the desired temperatures and cooled back to 4 K for spectral acquisition. For selected samples, photo-excitations were performed through a quartz window mounted on the assembly.

Phosphine (PH_3) was prepared according to the published protocols.[25] 3.4 g (0.041 mol) of dry crystalline phosphorous acid was placed in a 100 mL round-bottomed flask which was connected to a vacuum line. The flask was evacuated through three cold U-traps, and then slowly heated in an oil bath. The temperature of the flask maintained at 210 °C for about 30 minutes. Then the volatile products were separated by passing through three successive cold U-traps at −110, −120, and −196 °C. Pure PH_3 was retained in the last trap. For the D-labelling experiments, D-phosphorous acid was prepared according to the literature procedure by using PCl_3 and D_2O (99% D, Aldrich).[25] The quality of PH_3 was checked with gas phase IR spectroscopy (INSA OPTICS, FOLI10-R).

Structures and IR frequencies were calculated using B3LYP/6-311 + G(3df).[26,27] Calculated harmonic frequencies were scaled by a factor of 0.967.[28] Time-dependent TD-DFT[29,30] B3LYP/6-311 + G(3df) calculations were performed for the UV-Vis transitions. These calculations were carried out with Gaussian 16.[31] The NBO calculations were carried out with the version 6.0.[32] Bonding analysis was performed using the adaptive natural density partitioning (AdNDP) method.[33] The color-mapped AdNDP isosurface (0.5 au) graphs are rendered by the VMD 1.9.3 program.[34]

Acknowledgements

This work was supported by the National Natural Science Foundation of China (22025301, 21688102 and 22273012).

Conflict of Interest

The authors declare no conflict of interest.

Data Availability Statement

The data that support the findings of this study are available in the supplementary material of this article.

Keywords: boron · matrix isolation · multiple bonding · phosphorus · vibrational spectroscopy

[1] a) R. C. Fischer, P. P. Power, *Chem. Rev.* **2010**, *110*, 3877–3923; b) F. Dankert, C. Hering-Junghans, *Chem. Commun.* **2022**, *58*, 1242–1262; c) R. Borthakur, V. Chandrasekhar, *Coord. Chem. Rev.* **2021**, *429*, 213647; d) A. Staubitz, J. Hoffmann, P. Gliese, in *Smart Inorganic Polymers*, Eds E. Hey-Hawkins, M. Hissler, Wiley-VCH Verlag GmbH & Co. KGaA: Weinheim, Germany, **2019**, pp. 17–39.
[2] J. Feld, D. W. N. Wilson, J. M. Goicoechea, *Angew. Chem. Int. Ed.* **2021**, *60*, 22057–22061; *Angew. Chem.* **2021**, *133*, 22228–22232.
[3] a) M. Zhou, N. Tsumori, Z. Li, K. Fan, L. Andrews, Q. Xu, *J. Am. Chem. Soc.* **2002**, *124*, 12936–12937; b) H. Braunschweig, R. D. Dewhurst, K. Hammond, J. Mies, K. Radacki, A. Vargas, *Science* **2012**, *336*, 1420–1422.
[4] E. R. Lory, R. F. Porter, *J. Am. Chem. Soc.* **1973**, *95*, 1766–1770.
[5] a) C. A. Thompson, L. Andrews, *J. Am. Chem. Soc.* **1995**, *117*, 10125–10126; b) C. A. Thompson, L. Andrews, J. M. L. Martin, J. El-Yazal, *J. Phys. Chem.* **1995**, *99*, 13839–13849.
[6] P. Paetzold, A. Richter, T. Thijssen, S. Würtenberg, *Chem. Ber.* **1979**, *112*, 3811–3827.
[7] a) P. Paetzold, in *Advances in Inorganic Chemistry, Vol. 31* (Eds.: H. J. Emeléus, A. G. Sharpe), Academic Press, **1987**, pp. 123–170; b) J. Wang, P. Jia, W. Sun, Y. Wei, Z. Lin, Q. Ye, *Inorg. Chem.* **2022**, *61*, 8879–8886.
[8] a) S. Hagspiel, F. Fantuzzi, R. D. Dewhurst, A. Gärtner, F. Lindl, A. Lamprecht, H. Braunschweig, *Angew. Chem. Int. Ed.* **2021**, *60*, 13666–13670; *Angew. Chem.* **2021**, *133*, 13780–13784; b) J. A. Bailey, P. G. Pringle, *Coord. Chem. Rev.* **2015**, *297–298*, 77–90; c) A. N. Price, G. S. Nichol, M. J. Cowley, *Angew. Chem. Int. Ed.* **2017**, *129*, 10085–10089; d) E. Rivard, W. A. Merrill, J. C. Fettinger, P. P. Power, *Chem. Commun.* **2006**, 3800–3802; e) A. M. Borys, E. F. Rice, G. S. Nichol, M. J. Cowley, *J. Am. Chem. Soc.* **2021**, *143*, 14065–14070; f) A. Koner, B. Morgenstern, D. M. Andrada, *Angew. Chem. Int. Ed.* **2022**, *61*, e202203345.
[9] J.-S. Lu, M.-C. Yang, M.-D. Su, *Phys. Chem. Chem. Phys.* **2017**, *19*, 8026–8033.
[10] A. M. Arif, J. E. Boggs, A. H. Cowley, J. G. Lee, M. Pakulski, J. M. Power, *J. Am. Chem. Soc.* **1986**, *108*, 6083–6084.
[11] T. Jian, L. F. Cheung, T.-T. Chen, L.-S. Wang, *Angew. Chem. Int. Ed.* **2017**, *56*, 9551–9555; *Angew. Chem.* **2017**, *129*, 9679–9683.
[12] A. N. Price, M. J. Cowley, *Chem. Eur. J.* **2016**, *22*, 6248–6252.
[13] a) J. D. Watts, L. C. Van Zant, *Chem. Phys. Lett.* **1996**, *251*, 119–124; b) J.-S. Lu, M.-C. Yang, M.-D. Su, *ACS Omega* **2018**, *3*, 76–85; c) J. Liang, Y. Duan, J. Bai, Z. Li, X. Wang, Q. Su, *Comput. Theor. Chem.* **2020**, *1185*, 112873.
[14] a) L. Andrews, H.-G. Cho, *Inorg. Chem.* **2016**, *55*, 8786–8793; b) H.-J. Himmel, A. J. Downs, T. M. Greene, *Inorg. Chem.* **2001**, *40*, 396–407; c) J. Glatthaar, G. Maier, *Angew. Chem. Int. Ed.* **2004**, *43*, 1294–1296; *Angew. Chem.* **2004**, *116*, 1314–1317.
[15] G. Wang, M. Zhou, *Int. Rev. Phys. Chem.* **2008**, *27*, 1–25.
[16] T. J. Tague Jr, L. Andrews, *J. Am. Chem. Soc.* **1994**, *116*, 4970–4976.
[17] a) P. Hassanzadeh, Y. Hannachi, L. Andrews, *J. Phys. Chem.* **1993**, *97*, 6418–6424.
[18] L. Wang, X. Li, X. Jiang, X. Zeng, M. Zhou, *J. Phys. Chem. Lett.* **2022**, *13*, 2619–2624.
[19] P. Pyykkö, M. Atsumi, *Chemistry* **2009**, *15*, 12770–12779.
[20] W.-Z. Li, Y.-W. Pei, C.-X. Sun, Q.-Z. Li, J.-B. Cheng, *Chem. Phys. Lett.* **2012**, *532*, 36–39.
[21] K. B. Wiberg, *Tetrahedron* **1968**, *24*, 1083–1096.
[22] a) I. Mayer, *Int. J. Quantum Chem.* **1984**, *26*, 151–154; b) I. Mayer, *Chem. Phys. Lett.* **1983**, *97*, 270–274.
[23] A.-L. Lawzer, T. Custer, J.-C. Guillemin, R. Kołos, *Angew. Chem. Int. Ed.* **2021**, *60*, 6400–6402; *Angew. Chem.* **2021**, *133*, 6470–6472.
[24] Y. R. Luo, Comprehensive Handbook of Chemical Bond Energies, CRC Press, Boca Raton, FL, **2007**.
[25] M. N. R. Ashfold, R. N. Dixon, R. J. Stickland, *Chem. Phys. Lett.* **1984**, *111*, 226–233.
[26] C. Lee, W. Yang, R. G. Parr, *Phys. Rev. B: Condens. Matter Mater. Phys.* **1988**, *37*, 785–789.
[27] A. D. Becke, *J. Chem. Phys.* **1993**, *98*, 5648–5652.
[28] M. P. Andersson, P. Uvdal, *J. Phys. Chem. A* **2005**, *109*, 2937–2941.
[29] R. E. Stratmann, G. E. Scuseria, M. J. Frisch, *J. Chem. Phys.* **1998**, *109*, 8218–8224.
[30] J. B. Foresman, M. Head-Gordon, J. A. Pople, M. J. Frisch, *J. Phys. Chem.* **1992**, *96*, 135–149.
[31] Gaussian 16, Revision A.03, M. J. Frisch, G. W. Trucks, H. B. Schlegel, G. E. Scuseria, M. A. Robb, J. R. Cheeseman, G. Scalmani, V. Barone, G. A. Petersson, H. Nakatsuji, X. Li, M. Caricato, A. V. Marenich, J. Bloino, B. G. Janesko, R. Gomperts, B. Mennucci, H. P. Hratchian, J. V. Ortiz, A. F. Izmaylov, J. L. Sonnenberg, D. Williams-Young, F. Ding, F. Lipparini, F. Egidi, J. Goings, B. Peng, A. Petrone, T. Henderson, D. Ranasinghe, V. G. Zakrzewski, J. Gao, N. Rega, G. Zheng, W. Liang, M. Hada, M. Ehara, K. Toyota, R. Fukuda, J. Hasegawa, M. Ishida, T. Nakajima, Y. Honda, O. Kitao, H. Nakai, T. Vreven, K. Throssell, J. A. Montgomery, Jr., J. E. Peralta, F. Ogliaro, M. J. Bearpark, J. J. Heyd, E. N. Brothers, K. N. Kudin, V. N. Staroverov, T. A. Keith, R. Kobayashi, J. Normand, K. Raghavachari, A. P. Rendell, J. C. Burant, S. S. Iyengar, J. Tomasi, M. Cossi, J. M. Millam, M. Klene, C. Adamo, R. Cammi, J. W. Ochterski, R. L. Martin, K. Morokuma, O. Farkas, J. B. Foresman, D. J. Fox, Gaussian, Inc., Wallingford CT, **2016**.
[32] E. D. Glendening, C. R. Landis, F. Weinhold, *J. Comput. Chem.* **2013**, *34*, 1429–1437.
[33] D. Y. Zubarev, A. I. Boldyrev, *Phys. Chem. Chem. Phys.* **2008**, *10*, 5207–5217.
[34] W. Humphrey, A. Dalke, K. Schulten, *J. Mol. Graphics* **1996**, *14*, 33–38.

Manuscript received: November 28, 2022
Accepted manuscript online: December 23, 2022
Version of record online: February 16, 2023